JMEPEG (2010) 19:1183–1188
DOI: 10.1007/s11665-009-9588-2

1059-9495/$19.00

Nano SiC-Nickel Composite Coatings from a Sulfamat Bath Using Direct Current and Pulsed Direct Current

G. Heidari, H. Tavakoli, and S.M. Mousavi Khoie

(Submitted October 6, 2009)

Composite plating is a method through which the fine particles of metallic or non-metallic compounds are co-deposited in a plated layer to improve surface properties such as lubrication, wear resistance, and corrosion resistance. In this study, nano-sized SiC particles were co-deposited with nickel from sulfamat bath using pulsed and direct currents. Scanning electron microscopy, microhardness, wear, and corrosion tests were carried out to characterize the coating properties. The results showed that microhardness, wear resistance, and corrosion resistance of Ni-SiC composite coatings increased compared to those of Ni films.

Keywords corrosion, electrodeposition, nanocomposite coatings, SiC, sulfamat bath, wear

1. Introduction

Electroplating method has been in wide-spread use during the past several decades owing to its simplicity, cost effectiveness, and low temperature. Nickel coatings have good properties such as corrosion and abrasion resistance that can supersede chromium-containing coatings. Chromium-containing coatings have been banned because of its environmental pollution effects. The reinforcement particles in nickel coatings can significantly improve mechanical, tribological, anticorrosion, and antioxidation properties. The improvement of coating properties depends on the nature, size, concentration, and distribution of particles. Also, bath composition, electroplating parameters such as current density, pH value, temperature, frequency, duty cycle, and waveform can affect the properties of coating (Ref 1-4). Metallic matrix composite is used as erosion and corrosion resistance coatings, self-lubrication layers, and thermal barrier coatings, for example, in combustion engine and casting molds. The embedding of different solid particles in a metallic matrix can optimize mechanical, physical, electrical, piezo-electrical, or magnetic properties (Ref 3-10).

Electrodeposited composite coatings consist of nano- and micro-sized particles, which include hard oxide or carbide particles such as CeO_2, ZrO_2, Al_2O_3, SiC, WC, and diamond (Ref 1, 3, 5, 6, 9, 11, 12); metallic materials such as chromium; and polymer particles such as polytetrafluoroethylene (PTFE) (Ref 13).

In electroplating, three different kinds of current—direct current (DC), pulsed direct current (PDC), and pulsed reverse current (PRC), are usually used. Pulsed current plating has provided considerable advantages compared to DC plating (Ref 14).

G. Heidari, H. Tavakoli, and **S.M. Mousavi Khoie**, Mining and Metallurgical Department, Amirkabir University of Technology, P.O. Box 15875, 4413 Tehran, Iran. Contact e-mail: mmousavi@aut.ac.ir.

In pulse plating, a higher current density (I_p) can be achieved, also, in this technique the pulse parameters can change interface between a cathode and solution (Ref 15).

Chen et al. (Ref 16) investigated the influence of pulse frequency on the microstructure and wear resistance of co-deposited Ni-Al_2O_3 composite coating and showed that the frequency changes the texture and consequently changing the wear resistance. Hu and Chan (Ref 2) studied the morphology of Ni-SiC electrocomposite under a triangle waveform at different current density and found that nickel grain size decreased with increasing current density. Zimmerman et al. (Ref 17) have shown that microhardness values of pulsed electrodeposited coatings have been about two times higher than polycrystalline Ni-SiC composites.

In this article, morphological characteristics, hardness, wear, and corrosion resistance of Ni-SiC electrocomposite produced under PC and DC has been investigated.

2. Experimental

The nickel-nano (β-SiC) composite coatings were obtained from the electroplated sulfamat bath, whose composition and conditions are shown in Table 1.

The suspension of nano-composite (β-SiC with particle size 35 to 45 nm) and distilled water was stirred for 24 h and then added to nickel sulfamat bath solution. Then, the electroplating solution was stirred for 1 h using a magnetic stirrer and for another 30 min ultrasonically. The 200 mL plating solution was prepared and agitated by magnetic stirrer during electroplating to achieve homogeneous suspension. The pH value was controlled digitally. The particle size of the nano SiC was obtained by a FEG-TEM apparatus (Philips Co.). All XRD patterns were obtained by Bruker D8 apparatus. Figure 1 and 2 shows the XRD pattern and TEM image of β-SiC particles.

St12 steel ($30 \times 30 \times 1$ mm^3) was used as a cathode and a similar-sized nickel plate was used as an anode. Before electroplating, the substrate (cathode) was ground by 1200 grit SiC waterproof paper and then a sequence of cleaning was performed to remove contaminations. Different electroplating periods was used to obtain the same thickness (40 μm).

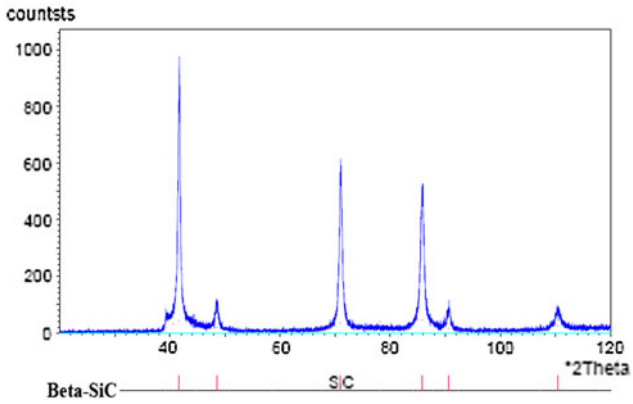

Fig. 1 XRD pattern of nano β-SiC particles

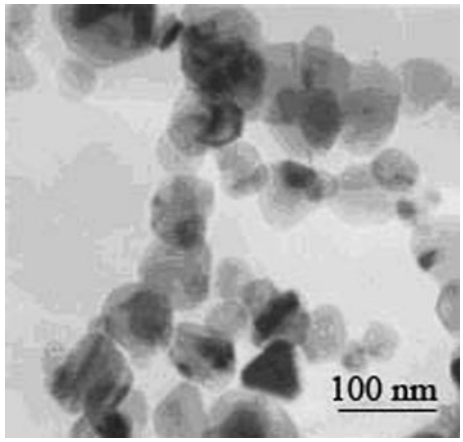

Fig. 2 TEM image of nano β-SiC particles

Table 1 Composition and condition of plating bath

Composition/Condition	Quantity
$Ni(SO_3NH_2)$	200 g/L
H_3BO_3	30 g/L
NiCl	10 g/L
Temperature	50 °C
pH	4

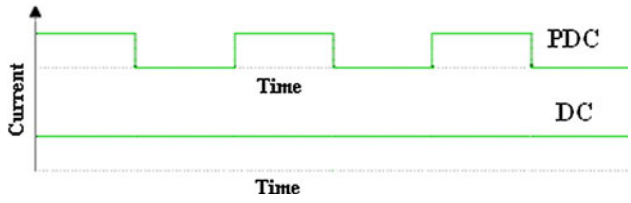

Fig. 3 A schematic of PDC and DC

Table 2 Electroplating conditions under DC and PDC

Electroplating bath	SiC concentration, g/L	Waveform of electroplating	Current shape	Duty cycle	Frequency, Hz
DC	···	DC	···	···	···
DC-SiC	30	DC	···	···	···
PDC	···	PDC	Rectangular	50%	100
PDC-SiC	30	PDC	Rectangular	50%	100

Electroplating coatings were obtained under DC and PDC according to Fig. 3 and Table 2.

The scanning electron micrograph was recorded with SEM XL30, and the amount of co-deposited SiC particles was determined using EDS coupled to the SEM at 10× magnification as an average of five measurements. Microhardness values were measured under the 15 g load and for 5 s. Final hardness value is an average of ten measurements. Wear tests were carried out by a pin-on-disc tribometer under the dry sliding wear according to Table 3.

Polarization curves were measured in a 3.5 wt.% NaCl solution at room temperature. The sweep rate of potential was set at 1 mV/s. The potential was changed from cathode to anode values in the range of E_0 −30 and E_0 +70 mV.

Table 3 Wear test conditions

Parameter	Selected value
Applied load, N	3
Test ball diameter, mm	6
Sliding distance, m	200
Velocity, m/s	0.1
Temperature, °C	25 ± 2
Environment	Air
Humidity, %	63 ± 5

3. Results and Discussion

3.1 Microstructure

Surface morphology of Ni-SiC composite coatings are shown in Fig. 4. As can be seen in these SEM micrographs, there are some differences between microstructures of the coatings. The nickel grain size is found to decrease as the waveform is changed from DC to PDC (Fig. 4a, c).

According to Fig. 4(a), the largest grain size of nickel obtained is about 7 μm; however, the largest grain size of nickel produced at PDC is about 4 μm. High current density can be achieved in pulsed plating compared to direct current (Ref 15). In theory of nucleation and growth of electrodeposits, a larger nucleation rate can be observed at a higher current density, while more extensive growth of nuclei is expected to take place at low current densities (Ref 18).

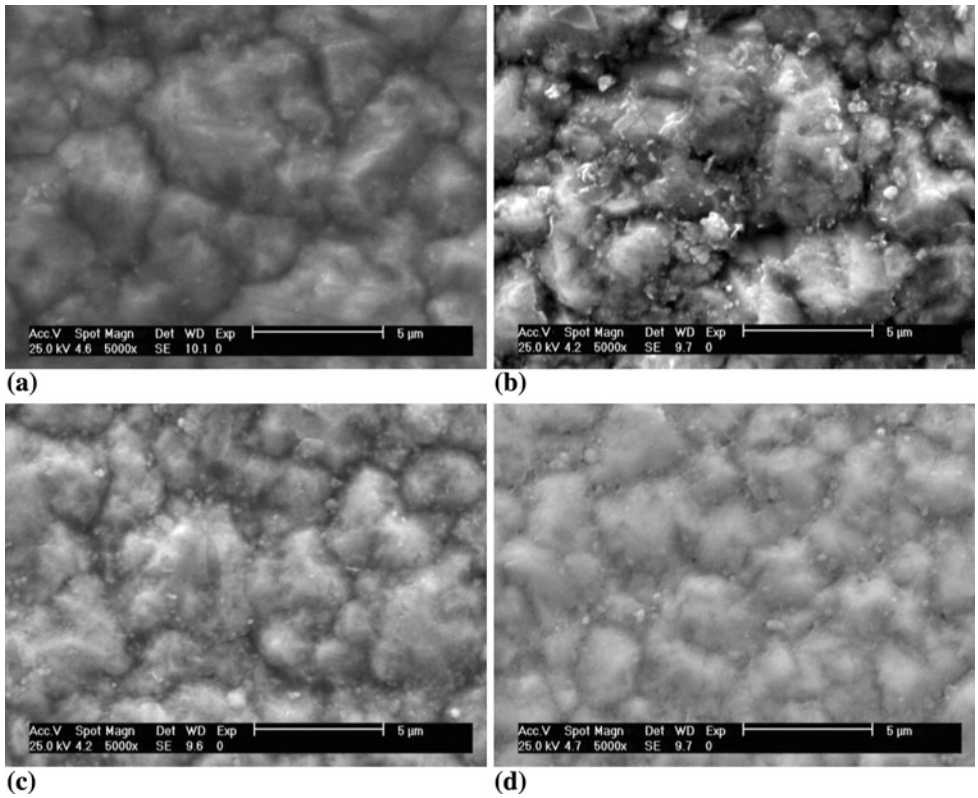

Fig. 4 SEM micrograph of pure Ni and composite coatings under DC and PDC: (a) DC; (b) DC-SiC; (c) PDC; and (d) PDC-SiC

Off-time of PDC leads to significant decrease in polarization concentration and hydrogen molecules concentration from cathode surface, which can result in increasing nickel ions concentration near the cathode surface. The increasing of nickel ions concentration increases nucleation rate. Therefore, higher nucleation rate under PDC than DC can develop smaller grains (Ref 19).

The distribution of SiC particles (white particles) are affected by the applied waveform. Agglomeration of SiC particles are observed on the composite coatings produced at DC (Fig. 4b). SiC particles are found to be homogeneously distributed in the composite coatings produced at PDC (Fig. 4d). At high current density, the rate of dissolution of anode is increased; therefore, the concentration of nickel ions near the cathode surface is also increased.

Increasing nickel ions concentration near the cathode surface results in increasing the repulsive forces among nickel ions with SiC particles adsorbed on the cathode surface. Thus, SiC particles can be more dispersive on the composite coating and agglomeration of SiC can hardly occur.

The co-deposition of SiC particles under DC and PDC is shown in Fig. 6. During the on-time of PDC, the nickel ions have higher chance to deposit, whereas during the off-time of PDC both the nickel ions and SiC particles have the same chance to deposit in the coating. Therefore, the SiC co-deposition under PDC is more than DC (Ref 16).

3.2 Microhardness

It is known that hardness of composite relates to matrix grain size and the distribution of reinforcement particles. As it is shown in Fig. 5, the microhardness of coatings under PDC is higher than the coatings under DC, which can be attributed to the smaller grains in these kinds of coatings. According to the Hall-Petch rule, the smaller grain size leads to higher hardness (Ref 17).

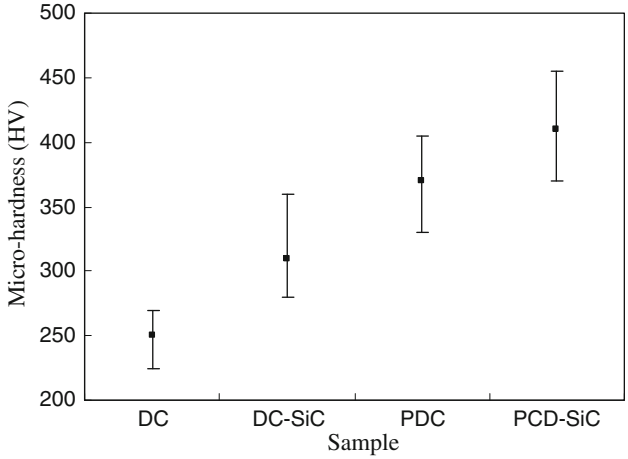

Fig. 5 The microhardness of coatings under different kind of currents

Also, microhardness of coatings with 30 g/L SiC in bath leads to higher hardness in comparison to coatings without SiC in bath, which can be attributed to the dispersion hardening mechanism (Ref 17). It is clear that as reinforcement particles have high hardness and strength, they will inhibit the plastic deformation of the soft nickel matrix and, therefore, increase the hardness of composite coating (Ref 20).

As it is shown in Fig. 5, the smaller grain size under PDC makes higher hardness than SiC particle in DC-SiC sample. Hence, smaller grain has higher contribution to hardness of coating than SiC particle.

3.3 Friction and Wear Behaviors

Friction behaviors for both different waveforms and coating composition are plotted in Fig. 6. It is known that the friction force or coefficient is increased rapidly during the running-in period of friction. However, this period is very short and severe wear occur at this period. After this period, friction force decreases to nearly constant value, with small changes in friction coefficients obtained under the same condition being arranged at 0.56 for DC, 0.53 for DC with nano SiC reinforcement, 0.42 for PDC, and 0.39 for PDC with nano SiC reinforcement.

It can be understood that the lowest friction coefficient is obtained with PDC with nano SiC reinforcement, followed by PDC, DC-SiC, and DC coatings, and these values imply that the frictional coefficient depends on surface hardness. However, it can be mentioned as a general rule that the coefficient depends on surface roughness and applied load (Ref 21).

Figure 7 presents the wear weight loss curve for four different coatings mentioned above. As can be seen from

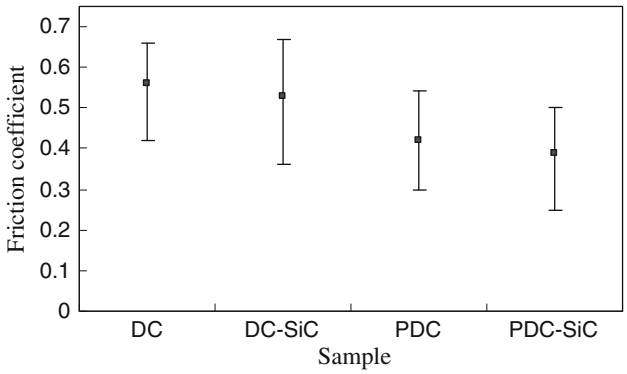

Fig. 6 Friction coefficient of pure Ni and Ni-SiC composite coatings under DC and PDC

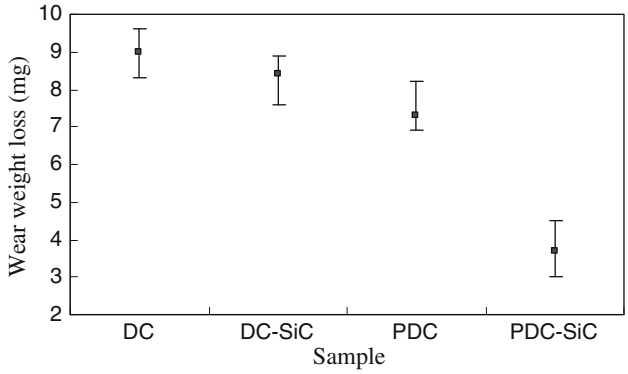

Fig. 7 Wear weight loss of pure Ni and Ni-SiC composite coatings under DC and PDC

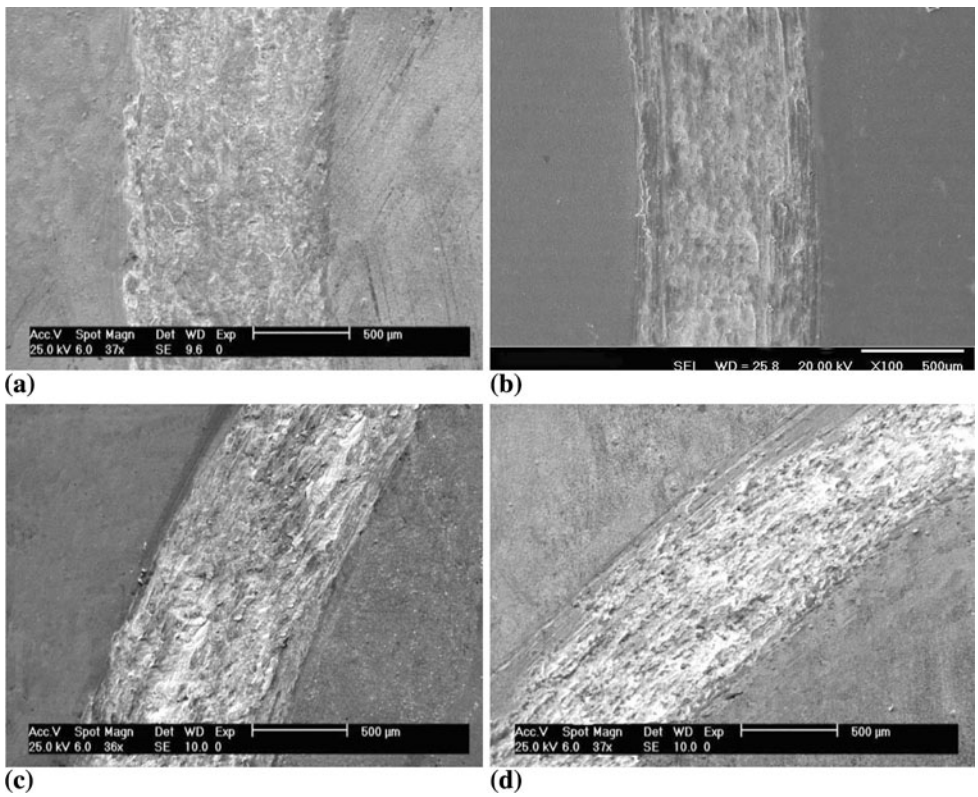

Fig. 8 SEM micrograph of wear surface of pure Ni and composite coatings under DC and PDC: (a) DC; (b) DC-SiC; (c) PDC; and (d) PDC-SiC

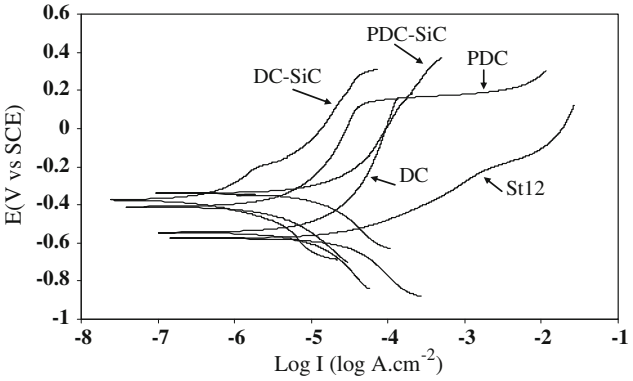

Fig. 9 Polarization curves of pure Ni and Ni-SiC composite coatings under DC and PDC and St12 substrate steel

Table 4 Corrosion current density and corrosion potential and corrosion rate of pure Ni and Ni-SiC composite coatings under DC and PDC and St12 substrate steel

Sample	I_{corr}, (A/cm^2) × 10^6	E_{corr}, V	Corrosion rate, mm/year
DC	5.33	−0.55	0.11
DC-SI	3.27	−0.4	0.07
PDC	4.86	−0.41	0.1
PDC-SiC	0.412	−0.33	0.009
St12	18.8	−0.58	0.406

Fig. 7, wear weight loss of coating under PDC is lower than the coating under DC. Also, the wear weight loss of SiC-Ni composite coating is lower than the pure nickel coating. Therefore, the wear resistance of coating under PDC is more than the coating under DC and the wear resistance of composite coating is more than the pure nickel coating. Co-deposition of SiC particles makes hardened coatings and leads to higher wear resistance coatings (Ref 22). Coatings under PDC have smaller grain size and lead to hardened coatings and higher wear resistance coating. According to the SEM micrograph, the wear mechanism is adhesive, as shown in Fig. 8.

3.4 Corrosion Properties

Polarization curves and corrosion parameters of samples are shown in Fig. 9 and Table 4. According to the polarization curves, the corrosion resistance of DC, DC-SiC, PDC, and PDC-SiC coatings is increased, respectively. PDC increases nucleation rate and results in smaller grain size. Since the preferred route of corrosion is grain boundary, the smaller grain size gives the longer corrosion route to the substrate. Therefore, the pulsed current leads to higher corrosion resistance coatings.

Nano SiC particles settle intercrystalline and intracrystalline in the microstructure, thus obstructing the corrosion path. In spite of this, the SiC particles in the coating decrease the contact area of corrosion medium with nickel and reduce the residual stress. Therefore, SiC particles in composite coatings increase the corrosion resistance compared to the pure nickel coatings (Ref 22).

4. Conclusions

The mechanical and corrosion behavior of nano SiC-nickel composite coatings from a sulfamat bath using DC and PDC have been studied and following conclusions can be assumed:

(a) The nickel grain size is found to decrease as the waveform is changed from DC to PDC.
(b) Agglomeration of SiC particles are observed on the composite coatings produced at DC.
(c) The microhardness of coatings under PDC is higher than the coatings under DC, which can be attributed to the smaller grains in these kinds of coatings.
(d) The lowest friction coefficient is obtained with PDC with nano SiC reinforcement.
(e) The wear weight loss of SiC-Ni composite coating is lower than the pure nickel coating.
(f) The pulsed current leads to higher corrosion resistance coatings compared to direct current.

References

1. L. Chen, L. Wang, Z. Zeng, and J. Zhang, Effect of Surfactant on the Electrodeposition and Wear Resistance of Ni-Al_2O_3 Composite Coatings, *Mater. Sci. Eng. A*, 2006, **434**, p 319-325
2. F. Hu and K.C. Chan, Deposition Behaviour and Morphology of Ni-SiC Electro-Composites Under Triangular Waveform, *Appl. Surf. Sci.*, 2005, **243**, p 251-258
3. S.T. Aruna, C.N. Bindu, V. Ezhil Selvi, V.K. William Grips, and K.S. Rajam, Synthesis and Properties of Electrodeposited Ni/Ceria Nanocomposite Coatings, *Surf. Coat. Technol.*, 2006, **200**, p 6871-6880
4. P. Gyftou, M. Stroumbouli, E.A. Pavlatou, P. Asimidis, and N. Spyrellis, Tribological Study of Ni Matrix Composite Coatings Containing Nano and Micro SiC Particles, *Electrochim. Acta*, 2005, **50**, p 4544-4550
5. Y. Zhou, H. Zhang, and B. Qian, Friction and Wear Properties of the Co-Deposited Ni-SiC Nanocomposite Coating, *Appl. Surf. Sci.*, 2007, **253**, p 8335-8339
6. A.S.M.A. Haseeb, U. Albers, and K. Bade, Friction and Wear Characteristics of Electrodeposited Nanocrystalline Nickel-Tungsten Alloy Films, *Wear*, 2008, **264**, p 106-112
7. L. Burzyńska, E. Rudnik, J. Koza, L. Błaż, and W. Szymański, Electrodeposition and Heat Treatment of Nickel/Silicon Carbide Composites, *Surf. Coat. Technol.*, 2008, **202**, p 2545-2556
8. H.K. Lee, H.Y. Lee, and J.M. Jeon, Codeposition of Micro- and Nano-Sized SiC Particles in the Nickel Matrix Composite Coatings Obtained by Electroplating, *Surf. Coat. Technol.*, 2007, **201**, p 4711-4717
9. S.C. Wang, W. Cheng, and J. Wei, Kinetics of Electroplating Process of Nano-Sized Ceramic Particle/Ni Composite, *Mater. Chem. Phys.*, 2003, **78**, p 574-580
10. N.S. Qu, D. Zhu, and K.C. Chan, Fabrication of Ni-CeO_2 Nanocomposite by Electrodeposition, *Scripta Mater.*, 2006, **54**, p 1421-1425
11. E.C. Lee and J.W. Choi, A Study on the Mechanism of Formation of Electrocodeposited Ni-Diamond Coatings, *Surf. Coat. Technol.*, 2001, **148**, p 234-240
12. F. Hou, W. Wang, and H. Guo, Effect of the Dispersibility of ZrO_2 Nanoparticles in Ni-ZrO_2 Electroplated Nanocomposite Coatings on the Mechanical Properties of Nanocomposite Coatings, *Appl. Surf. Sci.*, 2006, **252**, p 3812-3817
13. P. Bercot, E.P. Muñoz, and J. Pagetti, Electrolytic Composite Ni-PTFE Coatings: An Adaptation of Guglielmi's Model for the Phenomena of Incorporation, *Surf. Coat. Technol.*, 2002, **157**, p 282-289
14. C.T.J. Low, R.G.A. Wills, and F.C. Walsh, Electrodeposition of Composite Coatings Containing Nanoparticles in a Metal Deposit, *Surf. Coat. Technol.*, 2006, **201**, p 371-383
15. F.Y. Ge, S.K. Xu, S.B. Yao, and S.M. Zhou, Study of the Structures of Pulse Plating Zn-Fe Deposits, *Surf. Coat. Technol.*, 1996, **88**, p 1-4

16. L. Chen, L. Wang, Z. Zeng, and T. Xu, Influence of Pulse Frequency on the Microstructure and Wear Resistance of Electrodeposited Ni-Al_2O_3 Composite Coatings, *Surf. Coat. Technol.*, 2006, **201**, p 599-605
17. A.F. Zimmerman, D.G. Clark, K.T. Aust, and U. Erb, Pulse Electrodeposition of Ni-SiC Nanocomposite, *Mater. Lett.*, 2002, **52**, p 85-90
18. M. Cerisier, C.V. Haesendonch, and J.P. Celis, Morphology of Nanometer-Thick Electrolytic Copper Layers Investigated by Atomic Force Microscopy, *J. Electrochem. Soc.*, 1999, **146**(5), p 1829-1834
19. A.M. El-Sherik, U. Erb, and J. Page, Microstructural Evolution in Pulse Plated Nickel Electrodeposits, *Surf. Coat. Technol.*, 1997, **88**, p 70-78
20. I. Garcia, J. Fransaer, and J.P. Celis, Electrodeposition and Sliding Wear Resistance of Nickel Composite Coatings Containing Micron and Submicron SiC Particles, *Surf. Coat. Technol.*, 2001, **148**, p 171-178
21. I. Ozbek and C. Bindal, Mechanical Properties of Boronized AISI, W4 Steel, *Surf. Coat. Technol.*, 2002, **154**, p 14-20
22. I. Garcia, A. Conde, G. Langelaan, J. Fransaer, and J.P. Celis, Improved Corrosion Resistance Through Microstructural Modifications Induced by Codepositing SiC-Particles with Electrolytic Nickel, *Corros. Sci.*, 2003, **45**, p 1173-1189